Pedosphere **31**(2): 332–341, 2021
doi:10.1016/S1002-0160(20)60068-6
ISSN 1002-0160/CN 32-1315/P

Published by Elsevier B.V. and Science Press

PEDOSPHERE

www.elsevier.com/locate/pedosphere

Characteristics of greenhouse gas emissions from rice paddy fields in South Korea under climate change scenario RCP-8.5 using the DNDC model

Wonjae HWANG, Chanyang KIM, Kijong CHO and Seunghun HYUN*

Department of Environmental Science and Ecological Engineering, Korea University, Seoul 02841 (South Korea)

(Received July 7, 2020; revised August 21, 2020)

ABSTRACT

Understanding the greenhouse gas (GHG) emission from rice paddy fields is essential to come up with appropriate countermeasure in response to global warming. However, GHG emissions from paddy fields in South Korea are not well characterized. The objectives of this study were to estimate the carbon dioxide (CO_2) and methane (CH_4) emissions from rice paddy fields in South Korea, under the Representative Concentration Pathway 8.5 (RCP-8.5) climate change scenario using the DNDC (*i.e.*, DeNitrification-DeComposition) model at 1-km^2 resolution. The performance of the model was verified with field data collected using a closed chamber, which supports the application of the model to South Korea. Both the model predictions and field measurements showed that most ($> 95\%$) GHG emissions occur in the cropping period, between April and October. As a baseline (assuming no climate change), the national sums of the CO_2 and CH_4 emissions for the 2020s and 2090s were estimated to be 5.8×10^6 and 6.0×10^6 t CO_2-equivalents (CO_2-eq) year^{-1} for CO_2 and 6.4×10^6 and 6.6×10^6 t CO_2-eq year^{-1} for CH_4, respectively, indicating no significant changes over 80 years. Under RCP-8.5, in the 2090s, CH_4 emissions were predicted to increase by 10.7×10^6 and 14.9×10^6 t CO_2-eq year^{-1}, for a 10- or 30-cm tillage depth, respectively. However, the CO_2 emissions gradually decreased with rising temperatures, due to reduced root respiration. Deep tillage increased the emissions of both GHGs, with a more pronounced effect for CH_4 than CO_2. Intermittent drainage in the middle of the cropping season can attenuate the CH_4 emissions from paddy fields. The findings of this work will aid in developing nationwide policies on agricultural land management in the face of climate change.

Key Words: CH_4, CO_2, model performance, paddy soil, rising temperature, tillage depth

Citation: Hwang W, Kim C, Cho K, Hyun S. 2021. Characteristics of greenhouse gas emissions from rice paddy fields in South Korea under climate change scenario RCP-8.5 using the DNDC model. *Pedosphere*. **31**(2): 332–341.

INTRODUCTION

According to the Fifth Assessment Report of the Intergovernmental Panel on Climate Change (IPCC), the global atmospheric carbon dioxide (CO_2) concentration in 2011 was 391 μmol mol^{-1}, approximately 40% higher than the pre-industrial level in 1750. The Earth's annual average temperature had risen by 0.85 °C for the 133 years between 1880 and 2012 (IPCC, 2013). The major greenhouse gases (GHGs) affecting temperature rise are CO_2, methane (CH_4), and nitrous oxide (N_2O), all of which are predominantly emitted from anthropogenic processes in the industrial and agricultural sectors. Global anthropogenic GHG emissions from arable land through agricultural activities are estimated at 13.5% of the total emissions (IPCC, 2007).

Rice (*Oryza sativa* L.) is a highly important food crop that feeds more than 50% of the world's population (Zhou and Sun, 2017). Currently, Asia accounts for approximately 91% of the global rice growing area and 88% of global rice production (FAO, 2012). Flooded rice paddies are considered a significant anthropogenic source of CH_4 because of the favorable anaerobic conditions for the growth of methanogens (IPCC, 2013). Moreover, CH_4 is 28 times more powerful than CO_2, in terms of the global warming potential (GWP). Both soil properties and local meteorological conditions, such as the soil organic carbon (SOC), clay content, temperature, and moisture, are known to affect CH_4 emissions from paddy fields (Le Mer and Roger, 2001). The emission of CO_2 through soil microbial respiration from cultivated land is also significant (Davidson and Janssens, 2006). Common agronomic practices, such as tillage, can facilitate SOC oxidation (Osunbitan *et al*., 2005) by enhancing the oxygen (O_2) supply in paddy fields (Huang *et al*., 2016).

South Korea's agricultural area is small, with most cultivated lands sporadically distributed across the country (KOSIS, 2012). When a predictive model is performed at a large scale (*e.g*., 12.5 km^2), there is high uncertainty due to the associated inaccuracy with dispersed and small sized land. For this reason, it is necessary to perform model simulation with a high resolution (*e.g*., 1 km^2), based on high-resolution weather and soil data, to more precisely estimate the total national GHG emissions from South Korea.

So far, many process-based models, such as DNDC (*i.e*., DeNitrification-DeComposition), DAYCENT (*i.e*., Daily

*Corresponding author. E-mail: soilhyun@korea.ac.kr.

Century), and COUP (*i.e.*, Coupled Heat and Mass Transfer), have been developed to estimate GHG emissions in different countries (Li *et al*., 1992; Parton *et al*., 1996; Jansson and Moon, 2001). The DNDC model presents a technical advantage over other models because it can simultaneously estimate the daily CO_2, CH_4, and N_2O emissions from cultivated land such as rice paddies as affected by various agronomic practices (Li *et al*., 2011). To utilize DNDC as a successful predictive tool, the results of the model prediction must be verified using field measurements. In many countries (*e.g*., Australia, China, India, and USA), the verification of the DNDC model has been conducted by utilizing long-term field data under various local environmental conditions and comparing the data to the model (Li *et al*., 2011). In South Korea, however, few attempts have been made to verify the performance of the DNDC model using field measurements. A recent exception was the case of Chun *et al*. (2016), who conducted a comparative study of the CH_4 emissions between the model prediction and a single field measurement in a paddy field in Jeolla Province. In addition, the prediction of GHG emissions with a high-resolution (*e.g*., 1 km^2), at a nation-wide scale, has yet to be performed in South Korea.

Therefore, the objectives of this study were to i) simulate emissions of two GHGs (CO_2 and CH_4) of from rice paddy fields in South Korea using the DNDC model with a resolution of 1 km^2, ii) validate the model results through two-year field measurements of the GHG emissions, and iii) evaluate the effect of tillage depth (10 and 30 cm) and flooding conditions (continuous and intermittent) under the Representative Concentration Pathway 8.5 (RCP-8.5) climate change scenario on the GHG emissions from rice paddy fields across the country.

MATERIALS AND METHODS

Model description

In this study, we used DNDC version 9.5 (http://www.dndc.sr.unh.edu/), which was developed in 2012. The DNDC model is a biogeochemical model based on the daily circulation of carbon (C) and nitrogen (N) in agricultural ecosystems (Li *et al*., 1992). This model can predict emissions of major GHGs, such as CO_2, CH_4, nitric oxide (NO), and N_2O, from the biochemical processes of C and N in agricultural ecosystem.

Site description and model input data

South Korea occupies the southern portion of the Korean Peninsula, which lies in 33°09′–38°45′ N and 124°54′–131°06′ E, with a total national land area of 100 019 km^2 (Fig. S1, see Supplementary Material for Fig. S1). The terrain of South Korea is rumpled and mostly mountainous (63%), with the arable lands primarily located in the west and southeast (KOSIS, 2012). For a 1-km^2 scale resolution, the shapefile format (1:50 000 scale) of the land use data was obtained from the Korea Ministry of Environment. The total paddy land was spilt into 63 808 1-km^2 grid cells. The total area of the paddy land, calculated by integrating its actual coverage over the 63 808 grid cells, was approximately 12 600 km^2 (about 13% of the total national land area).

To identify the regional differences in the input data (climate and soil) and GHG (*e.g*., CO_2 and CH_4) emissions, the range was expressed based on five administrative districts, Chungcheong, Gangwon, Gyeonggi, Gyeongsang, and Jeolla provinces. The geographical locations of the provinces are depicted in Fig. S1a.

The input data used in the DNDC model prediction are listed in Table I. For the meteorological data, the RCP-8.5 climate change scenario, based on the HadGEM3RA model, was used. RCP-8.5 is considered the 'high-end' case and is often used to simulate an extreme case of climate change. The daily maximum/minimum temperature (°C) and precipitation (mm) data that correspond to the RCP-scenario were obtained from the Korea Meteorological Administration (KMA) (http://climate.go.kr). The ranges of the climate data for each administrative district are shown in Fig. S2 (see Supplementary Material for Fig. S2). The baseline scenario

TABLE I

Input data for the DNDC (*i.e*., DeNitrification-DeComposition) model

Type	Sub-type	Unit	Scale	Source
			km^2	
Climate	Maximum temperature	°C	1	Korea Meteorological Administration
	Minimum temperature	°C	1	
	Precipitation	cm	1	
Agronomic practice	Tillage	cm	Default value	Korea Rural Development Administration
	Fertilization	kg N ha^{-1}	Default value	
	Cultivation period	d	Default value	
	Flooding	d	Default value	
Soil factor	Initial soil organic C	g kg^{-1}	1	Korea Rural Development Administration
	Clay	%	1	
	pH (1:5)		1	
	Bulk density	g cm^{-3}	1	

over the model prediction period, from 2016 to 2095, was set to the actual measured 2011 weather data. Climate data were obtained from 75 weather stations across the country in 2011 and then interpolated with a 1-km^2 grid cell using inverse distance weighting and kriging (Marchetti *et al*., 2012).

For the agronomic data, the common practices recommended by the Korea Rural Development Administration (KRDA) for rice cultivation were applied. The rice cultivation period was set from April 30 to October 21, and tillage was carried out on April 9. Fertilization was assumed to be at a rate of 50 kg N ha^{-1} before rice transplantation (April 8) and 20 kg N ha^{-1} in the middle of the growing season (July 28). As for an irrigation practice, initial continuous flooding from April 14 to July 17 and subsequent intermittent flooding at 5-d intervals from July 27 to September 26 were assumed. Model prediction was run for tillage depths of 10 and 30 cm (referred to as the 10T and 30T conditions, respectively).

The soil chemical data (*e.g*., initial SOC and pH) were obtained from a soil database of approximately 365 000 data points established by KRDA. The soil physical data (*e.g*., clay content and bulk density) were reprocessed at a spatial resolution of 1 km^2 on the basis of 377 domestic representative soil series from a 1:25 000 scale soil map. Approximately 61.4% of the soil properties were explained by actual measurements, while the remainder was estimated by interpolation with 1-km^2 grid cells through the Kriging method (Omran, 2012). The distribution of the soil data is shown in Fig. S2.

Following the 5-year spin-up period from 2011 to 2015, we performed an 80-year prediction from 2016 to 2095. The results of the GHG emissions for every ten-year period (2016–2025, 2026–2035, *etc*.) were averaged and referred to as the 2020s, 2030s, *etc*., respectively. Both CO_2 and CH_4 emissions were converted to CO_2-equivalents (CO_2-eq) using the reported values of specific global warming potentials. Thus, GHG emissions from paddy fields are expressed in t CO_2-eq ha^{-1} year^{-1}, unless otherwise noted.

Experimental site and basic input data collection for DNDC model verification

To validate the DNDC model prediction, CO_2 and CH_4 emissions were measured from a rice paddy field (37°35′1″ N, 127°14′16″ E) at the Korea University Agricultural Farm (Deokso field), located in Gyeonggi Province (Fig. S1). During January 2015 and November 2016, GHG emissions were measured approximately once a month (22 data points for CO_2 and 21 for CH_4). The average values of the minimum and maximum annual air temperature during the observation period were 7.7 and 18.9 °C, respectively, and the annual cumulative precipitation was 847 mm. The agronomic practices executed at the Deokso field are slightly different from KRDA recommendations as summarized in Table II. The cultivation period was from May 1 to October 21, with tillage carried out at a depth of 10 cm on April 10. For fertilization, 50 and 20 kg N ha^{-1} was applied on April 10 and July 29, respectively. Intermittent flooding was performed from April 15 to September 24, with 5-d intervals. To characterize the field soil, six composite samples were collected and selected properties (*e.g*., bulk density, clay, initial SOC, and pH) were determined.

TABLE II

Input data for the verification of the DNDC (*i.e*., DeNitrification-DeComposition) model from a rice paddy field at the Korea University Agricultural Farm

Variable	Value
Location	37°35′1″ N, 127°14′16″ E
Land use	Paddy (*Oryza sativa* L.)
Climate	
Daily maximum average temperature (°C)	18.9
Daily minimum average temperature (°C)	7.7
Annual precipitation (mm)	847
Agronomic practice	
Tillage (cm)	10 (April 10)
Fertilization (kg N ha^{-1})	50 (April 10) and 20 (July 29)
Cultivation period	May 1–October 21
Flooding period	April 15–September 24 (intermittent flooding)
Soil factor	
Soil organic C (%)	1.5
Clay (%)	15
pH (1:5)	5.6
Bulk density (g cm^{-3})	1.2

Measurement of CO_2 and CH_4 emissions

The GHG measurement system consisted of the closed chamber and the measuring unit in which a moisture filter, a direct current (DC) pump, a flow meter, a gas detector, and a data logger are sequentially connected (Fig. S1). The chamber was an opaque acrylic cylinder with a diameter of 30 cm, a height of 20 cm, and a volume of 25.1 L. During flux measurement, 5 cm of the anchor in the cylinder bottom was inserted into the soil. A closed chamber is designed to collect the gas emitted from the soil surface, according to the gas concentration gradient between the soil and chamber. This system detects the concentration change over time until the CO_2 and CH_4 concentrations reach steady states in the chamber (Malyan *et al*., 2016). The gas collected in the chamber is allowed to flow to the measuring unit through a 4-mm polyurethane tube and then circulate back to the chamber. The detector unit is composed of a CO_2 sensor (Soha-Tech, South Korea), with a detection range of 1–3 000 μmol mol^{-1}, and a CH_4 sensor (Axetris, Switzerland), with a detection range of 1–100 μmol mol^{-1}. The DC pump (Motorbank, South Korea) and the air flow meter (Dwyer, USA) were installed to maintain a constant gas

flow rate (*ca.* 1 L min^{-1}) of air between the chamber and the detector, thereby creating a continuous air circulation system. In the field, the measurements were repeated twice (*e.g.*, 8:00–11:00 a.m. and 3:00–6:00 p.m.) on a given day and the two measurements were used to obtain a daily average. Each measurement took approximately 3 h. Prior to the field measurements, the system was calibrated using CO_2 and CH_4 standard gas (N_2 balance, 11.0 MPa) at 500, 1 000, and 2 000 μmol mol^{-1} for CO_2 and 5, 10, and 50 μmol mol^{-1} for CH_4. The coefficients of determination were 0.999 and 0.991 for the CO_2 and CH_4 calibration curves, respectively.

The concentrations of CO_2 and CH_4 in the chamber were detected once per second and the gas flux (F, mg CO_2/CH_4 m^{-2} h^{-1}) was calculated using Eq. 1 (Malyan *et al.*, 2016):

$$F = \rho \times \frac{V}{A} \times \frac{\Delta C}{\Delta t} \times \frac{273}{T + 273} \quad (1)$$

where ρ is the density of the gas (mg m^{-3}), V is the volume of the chamber (m^3), A is the bottom area of the chamber (m^2), $\frac{\Delta C}{\Delta t}$ is the average rate of concentration change (μ mol mol^{-1} h^{-1}), and T is the average temperature in the chamber (°C).

Statistical analysis

To validate the DNDC model performance, the model efficiency (ME) and coefficient of determination (r^2) were employed as shown in Eqs. 2 and 3 (Vaezi, 2014):

$$\mathrm{ME} = 1 - \frac{\sum_{i=1}^{n} (P_i - M_i)^2}{\sum_{i=1}^{n} (M_i - \overline{M})^2} \quad (2)$$

$$r^2 = \left(\frac{\sum_{i=1}^{n} (M_i - \overline{M})(P_i - \overline{P})}{\sqrt{\sum_{i=1}^{n} (M_i - \overline{M})^2 \times \sum_{i=1}^{n} (P_i - \overline{P})^2}} \right)^2 \quad (3)$$

where P_i is the predicted value, M_i is the measured value, i is the number of measured values, and $\overline{P}$ and $\overline{M}$ are the means of the predicted and measured values, respectively.

RESULTS AND DISCUSSION

Field measurements and model prediction

The precipitation and air temperature data during the experimental period (January 2015–November 2016) are provided in Fig. 1a. The field measurements of CO_2 and CH_4 emissions (open circle) are shown in Fig. 1b, c, respectively, along with the results of the DNDC model prediction for the respective gas (closed circle). Information regarding the rice cultivation period, flooding/drainage, and the time points of tillage and fertilization are also given. For comparison, the results of the GHG emissions were converted to values in kg CO_2-eq ha^{-1} d^{-1}. Two points should be noted here. Firstly, the predicted emissions of CO_2 and CH_4 ranged 1.5–181.7 and 0.02–17.7 kg CO_2-eq ha^{-1} d^{-1}, respectively, both of which are quite similar to the field measurements. Secondly, for both the field and model data, the most ($> 85\%$) GHG emissions from paddy fields occurred during the cropping seasons (April–October). In particular, CH_4 emissions were negligible ($< 2.3\%$) during the non-cropping seasons.

The field measurements of the daily CO_2 emissions ranged 1.1–159.1 kg CO_2-eq ha^{-1} d^{-1} ($n = 22$), with a daily average of 37.4 kg CO_2-eq ha^{-1} d^{-1} over the two years (Fig. 1b). The average value is more than twice the value measured from a continuously flooded paddy field (*i.e.*, 15.0 kg CO_2-eq ha^{-1} d^{-1}) located in the Gyeongsang Province (Haque *et al.*, 2015). Note that the intermittent flooding method was employed in this work, in which 5-d-interval aerobic conditions were applied 20 times during the cropping season. Upon removal of the floodwater by drainage, the soil microbial respiration substantially increases, thereby producing more CO_2 (Aulakh *et al.*, 2001). Furthermore, the diffusive transport of CO_2 can be strongly enhanced under intermittent draining compared to continuous flooding (Hillel, 1998).

The average CO_2 emissions in May, just after rice transplanting, were 40.1 kg CO_2-eq ha^{-1} d^{-1}. This value is 5.1 times greater than that in March (7.8 kg CO_2-eq ha^{-1} d^{-1}). In particular, the emissions increased sharply from May to July, exhibiting a maximum of 159.1 kg CO_2-eq ha^{-1} d^{-1} in July, which is consistent with the rising pattern of average daily temperatures during this period. Soil temperature is known as an important climate factor affecting CO_2 emissions from soil (Huang *et al.*, 2016). With rising soil temperature, microbial enzymatic activity for SOC decomposition is enhanced and thus more CO_2 is generated (Davidson and Janssens, 2006) as long as the O_2 supply is sufficient enough to maintain the aerobic conditions.

The field measurements of the daily CH_4 emissions ranged 0.3–13.0 kg CO_2-eq ha^{-1} d^{-1} ($n = 21$), with a daily average of 2.9 kg CO_2-eq ha^{-1} d^{-1} for the two years (Fig. 1c). As described earlier, most of the CH_4 emissions occurred during the rice growing season from May to October, when the paddy field was intermittently flooded. Methanogenesis, which requires strict anaerobic conditions and low redox potentials (< -200 mV), is established when the paddy soil is submerged by floodwater during the rice growing season (Le Mer and Roger, 2001; Yang and Chang, 2001). In addition, CH_4 emissions are also influenced by the number and duration of drainage periods (Minamikawa *et al.*, 2014). Yang and Chang (2001) found that CH_4 emissions reduced when the redox potential was increased (up to -100 mV), through intermittent drainage after the extended duration of flooded conditions with a low (-200 mV) redox potential.

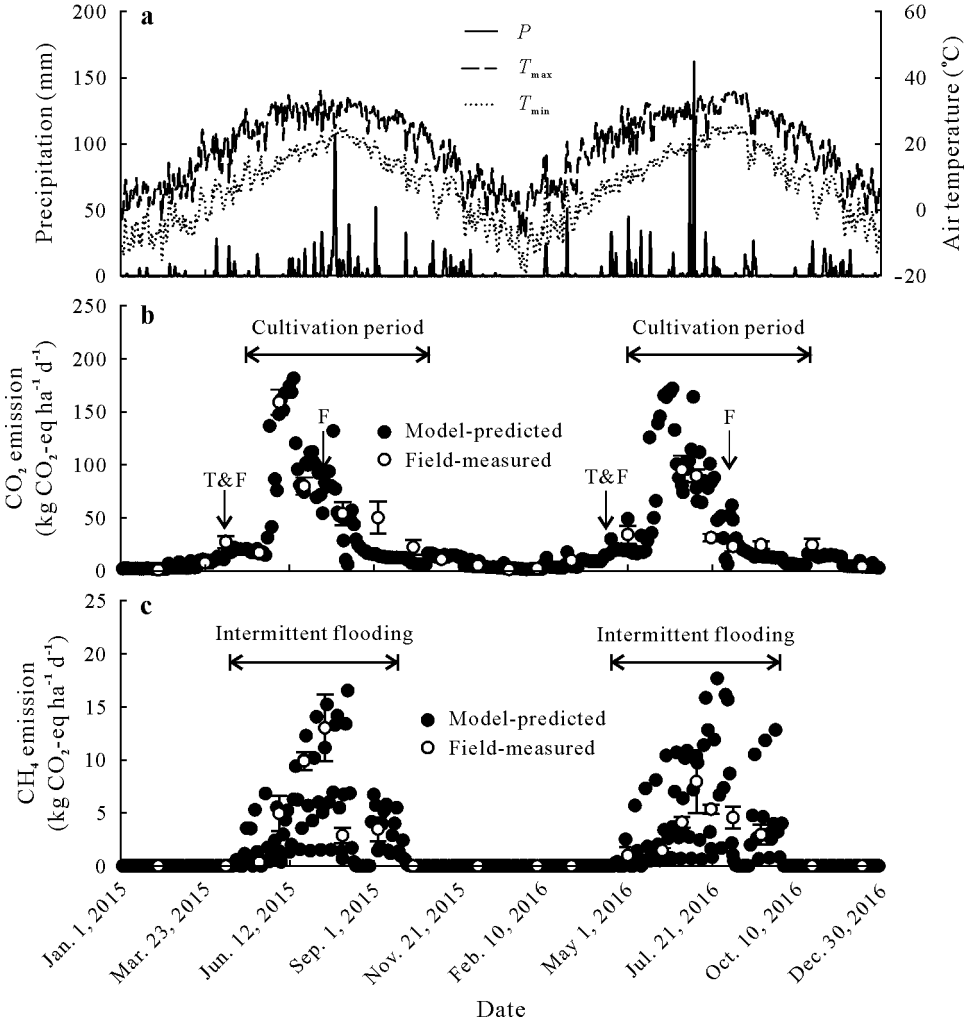

Fig. 1 Daily maximum and minimum air temperatures and precipitation during the experimental period (2015–2016) (a) and comparisons of the DNDC (*i.e.*, DeNitrification-DeComposition) model-predicted and field-measured CO_2 (b) and CH_4 (c) emissions from a rice paddy field in Deokso, South Korea. CO_2-eq = CO_2-equivalents; P = precipitation, $T_{\max}$ = maximum air temperature; $T_{\min}$ = minimum air temperature; T= tillage; F= fertilization.

When the soil is saturated by flooding after tillage operation, methanogenesis begins within 10–21 d when the soil redox potential decreases down to −200 mV or less (Le Mer and Roger, 2001). This trend is consistent with the prediction model in this study, as CH_4 emissions first occurred on the 14th day after flooding (Fig. 1). During this time, the reduced bulk density, caused by intensive tillage, would further promote CH_4 emissions. Facilitated transformation of SOC into dissolved organic C (DOC), which might develop during the initial 5–7 d of aerobic conditions, can likely exist in paddy soils more so in the case of deep tillage rather than shallow tillage just prior to the introduction of flooding (Le Mer and Roger, 2001; Snyder *et al.*, 2009).

For measurements performed in a continuously flooded Korean paddy field, Gutierrez *et al.* (2013) reported daily CH_4 emissions of 55.2 kg CO_2-eq ha^{-1} d^{-1} ($n = 6$) during the cropping season, which is more than four times the maximum daily value of 13.0 kg CO_2-eq ha^{-1} d^{-1} in this study. A similar flooding effect has been reported for other Asian paddy fields. For example, in a Japanese paddy field, annual CH_4 emission was reduced from 1.1 to 0.4t CO_2-eq ha^{-1} $year^{-1}$ after implementation of two drainage practices during the growing season (Minamikawa *et al.*, 2014).

Model verification

The field measurements of the CO_2 ($n = 22$) and CH_4 ($n = 21$) emissions were plotted with their respective model prediction in Fig. 2, along with the ME and r^2 values between the two datasets. The ME value is an analytical technique that compares the squared sum of the absolute error with that of the difference between the measured value and mean measured value (Eq. 2). The ME value has a range between $-\infty$ and 1. A value closer to 1 indicates a greater similarity between the measured and predicted values. The ME for CO_2 and CH_4 was 0.82 and 0.83, respectively. The r^2 value is the most commonly used regression coefficient, which indicates the ability of the model to explain variations in the measured

values (Eq. 3). The closer the r^2 value is to 1, the better the model matches the pattern of the measurements. The r^2 values for CO_2 and CH_4 are 0.82 and 0.86, respectively, at $P < 0.001$, indicating a strong agreement between the model prediction and field measurements.

Annual CO_2 and CH_4 emissions across South Korea

The data range of the model prediction (63 808 cells) of annual GHG emissions was presented in boxplots as a function of the administrative districts (Figs. 3 and 4). For a graphic view, GHG emissions are also depicted in Fig. S3 (see Supplementary Material for Fig. S3). The magnitude of emissions were grouped into 10 different classes and denoted by 10 different colors.

Regional variation according to administrative districts. In the 2020s, the average CO_2 emissions in the five administrative districts were in the order of Jeolla > Gyeongsang ≈ Gangwon > Chungcheong > Gyeonggi (Fig. 3), which is consistent with the initial SOC content used as the DNDC model input data. For Chungcheong and Gyeonggi, the CO_2 emissions were lower than the national average, which is likely due to their initial SOC contents. The average initial SOC contents in Chungcheong and Gyeonggi were 13.3 and 12.6 g kg^{-1}, respectively, both of which are lower than the national average of 14.2 g kg^{-1}.

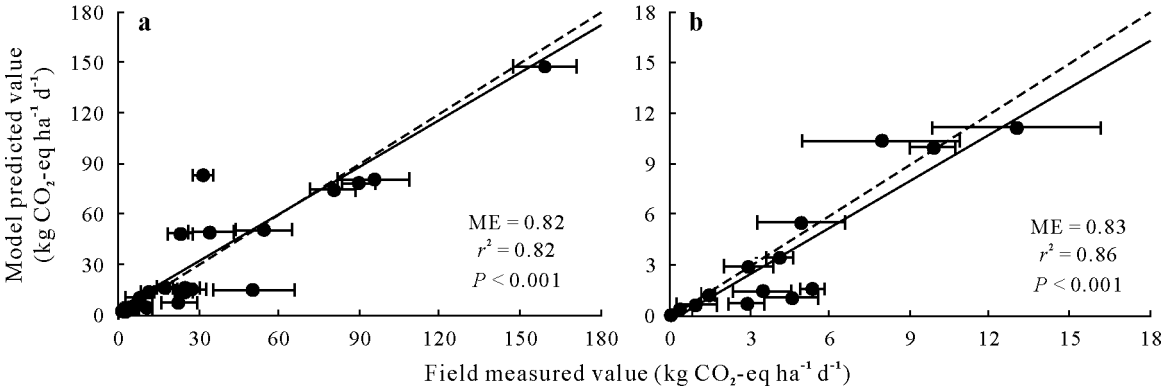

Fig. 2 Comparison between the DNDC (*i.e.*, DeNitrification-DeComposition) model-predicted and field-measured CO_2 (a) and CH_4 (b) emissions from a paddy field in Deokso, South Korea. The dotted lines are imaginary 1:1 lines. Data points of measured greenhouse gas emissions are the means of duplicates with the standard deviations as error bars. CO_2-eq = CO_2-equivalents; ME = model efficiency; r^2 = coefficient of determination.

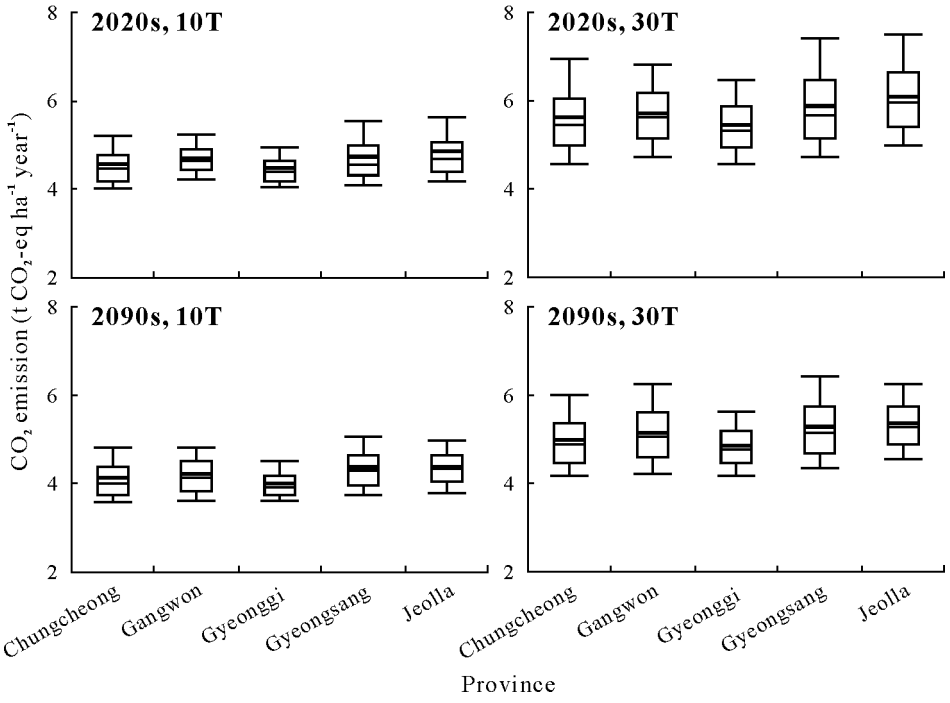

Fig. 3 Boxplots of CO_2 emissions from paddy fields with a 10-cm (10T) or 30-cm (30T) tillage depth predicted for five provinces in South Korea under the Representative Concentration Pathway 8.5 (RCP-8.5) scenario in the 2020s and 2090s using the DNDC (*i.e.*, DeNitrification-DeComposition) model. The lower and upper borders of each box represent the 25th and 75th percentiles, respectively, and the horizontal and bold horizontal lines within the box indicate the median and average values, respectively. CO_2-eq = CO_2-equivalents.

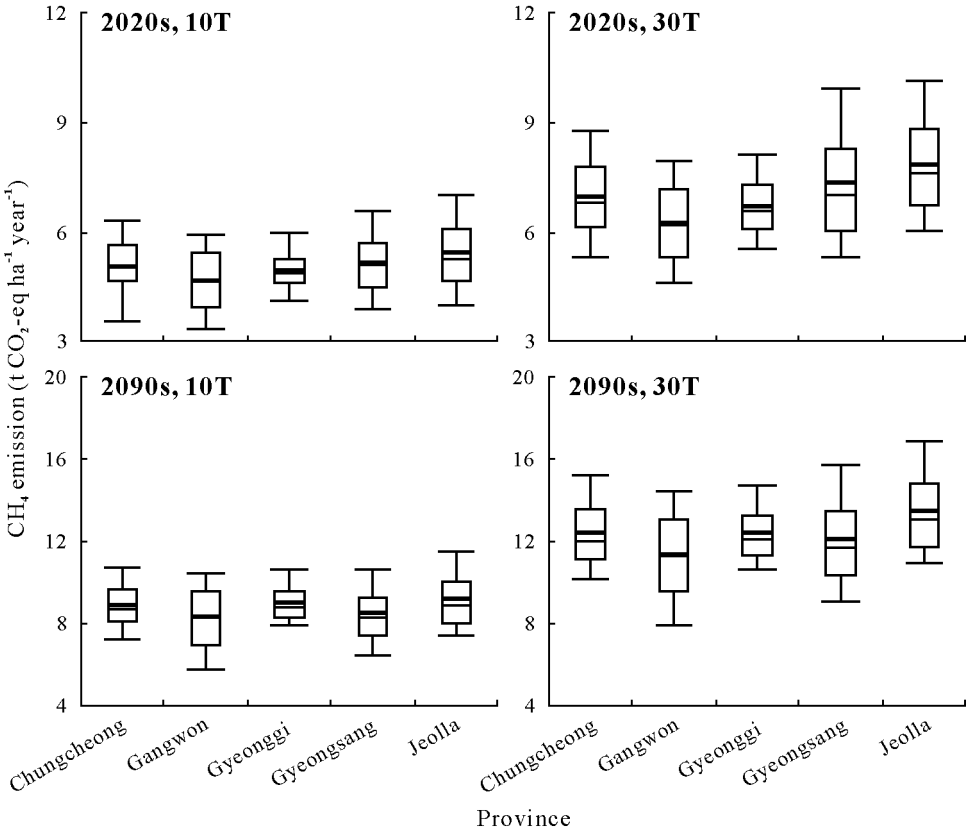

Fig. 4 Boxplots of CH_4 emissions from paddy fields with a 10-cm (10T) or 30-cm (30T) tillage depth predicted for five provinces in South Korea under the Representative Concentration Pathway 8.5 (RCP-8.5) scenario in the 2020s and 2090s using the DNDC (*i.e.*, DeNitrification-DeComposition) model. The lower and upper borders of each box represent the 25th and 75th percentiles, respectively, and the horizontal and bold horizontal lines within the box indicate the median and average values, respectively. CO_2-eq = CO_2-equivalents.

The sequence of the annual CO_2 emission remained unchanged until the 2090s, indicating that the level of SOC stocks was mainly responsible for the magnitude of the CO_2 emissions from paddy fields. The range of annual CO_2 emissions in the 2020s was between 3.9 and 5.6t CO_2-eq ha^{-1} $year^{-1}$, with a national average of 4.7t CO_2-eq ha^{-1} $year^{-1}$ (Fig. 3). These values were similar to the results of Pathak *et al*. (2005) who, using the DNDC model, in the 2010s estimated 2.2–8.8 kg of CO_2 emissions from paddy fields in India. In this study, the annual average of CO_2 emissions was slightly reduced to 4.3t CO_2-eq ha^{-1} $year^{-1}$ in the 2090s, which is consistent with the declining of the 10-cm depth SOC stocks from 17.6t C ha^{-1} in the 2020s to 16.1t C ha^{-1} in the 2090s (Fig. S4, see Supplementary Material for Fig. S4).

For the average annual CH_4 emissions in the 2020s, the order was Jeolla > Gyeongsang ≈ Chungcheong ≈ Gyeonggi > Gangwon, and the range of the data was between 3.3 and 7.0t CO_2-eq ha^{-1} $year^{-1}$, with a national average of 5.1t CO_2-eq ha^{-1} $year^{-1}$ (Fig. 4). Among the five districts, the average of Gangwon was the lowest at 4.6t CO_2-eq ha^{-1} $year^{-1}$. As shown in Fig. S2, the five districts showed significant variation in the annual temperature due to their geographic locations. In the DNDC model, the microbial activity of methanogens is assumed to increase exponentially with temperature rise (Fumoto *et al*., 2008). Thus, the low CH_4 emissions from Gangwon are most likely due to its lower annual temperatures (approximately 2 °C) than the national average for a given period. The annual averages of Gangwon were 10.1 °C and 14.4 °C for the 2020s and 2090s, respectively, whereas the national averages were 12.2 °C and 16.3 °C for the 2020s and 2090s, respectively.

Gutierrez *et al*. (2013) performed CH_4 emission measurements in eight different locations in South Korea between 2010 and 2011. Their results for the annual CH_4 emissions were between 5.1 and 12.6t CO_2-eq ha^{-1} $year^{-1}$, which are greater than the results in this work due to the continuous flooding practice employed in their study. However, CH_4 emissions estimated for Indian paddy fields ranged between 0.2 and 3.5t CO_2-eq ha^{-1} $year^{-1}$ (Pathak *et al*., 2005), which are approximately 70% less than the results found in this study. This difference was presumably due to the low SOC content (2.0–8.0 g kg^{-1}) in India, which is considerably lower than the average SOC (14.2 g kg^{-1}) in South Korea.

Effect of tillage depth. Tillage practices performed on agricultural lands can influence the physicochemical

properties of soils and level of GHG production (Le Mer and Roger, 2001). Intensive tillage can disrupt soil aggregates and promote SOC decomposition, which can lead to the formation of CO_2 or CH_4, depending upon the degree of the redox potential of the soil (Osunbitan *et al*., 2005; Snyder *et al*., 2009). In this study, the predicted emissions of both CO_2 and CH_4, from a given grid cell, with 30T were always higher than those with 10T.

The annual averages of CO_2 emissions under the 30T condition were 20.9%–25.9% higher than those under 10T across the administrative districts in the 2020s (Fig. 3). In the 2090s, the difference between these two conditions was 19.8%–24.3% due to the reduced SOC stocks by that time (Osunbitan *et al*., 2005). Note that the depletion of SOC in paddy fields was more pronounced at 30T, which decreased by 3.4t C ha^{-1} over 80 years (Fig. S4).

Meanwhile, the effect of tillage depth would be more apparent on CH_4 emissions. Across the five administrative districts, the CH_4 emissions under the 30T condition would be 34.8%–45.9% higher than those under 10T for the 2020s (Fig. 4). The CH_4 emissions under tillage effect would increase by 37.3%–47.1% in the 2090s when two synergetic effects from deep tillage (Snyder *et al*., 2009) and temperature rise (Le Mer and Roger, 2001) are occurring concurrently, even though the SOC levels were lower.

Temporal changes between the 2020s and 2090s. National emissions of CO_2 and CH_4 from entire paddy fields in South Korea are shown in Fig. 5 as a function of time (from the 2020s to 2090s). The baselines, assuming no climate change, are also shown as dotted lines (30T) or dashed lines (10T), both of which would not significantly vary during the observation period.

The national CO_2 emissions were predicted to steadily decline until the 2090s, mostly due to the reduction of SOC stocks under the RCP-8.5 scenario. With 10T tillage, CO_2 emissions in the 2020s would be 5.8×10^6 t CO_2-eq $year^{-1}$ and decrease by approximately 0.5×10^6 t CO_2-eq $year^{-1}$ until the 2090s. With 30T, CO_2 emissions in the 2020s were predicted to increase by 24.1% compared to those of the 10T scenario. As mentioned previously, for microorganisms, deep tillage can improve the accessibility of SOC on the surfaces of soil particles, thereby promoting oxidative degradation of SOC and producing more CO_2 (Osunbitan *et al*., 2005). As climate change proceeds until the 2090s, the CO_2 emissions for the 30 cm tillage practice would gradually reduce by 11.1% from 7.2×10^6 to 6.4×10^6 t CO_2-eq $year^{-1}$. The decrease in the root growth at a soil temperature above 25 °C may be attributed to the inhibition of the formation and elongation of the main roots (Arai-Sanoh *et al*., 2010). The inhibition of root growth will reduce the amount of oxygen diffused into the rhizosphere soil through the rice aerenchyma, which in turn causes a

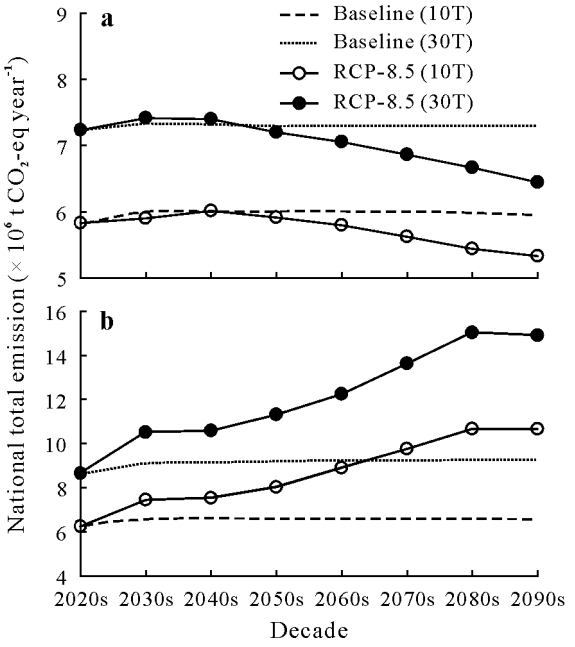

Fig. 5 Estimates of the total national CO_2 (a) and CH_4 (b) emissions from paddy fields with a 10-cm (10T) or 30-cm (30T) tillage depth for the 2020s–2090s under the Representative Concentration Pathway 8.5 (RCP-8.5) scenario in South Korea. The baseline emissions are estimated based on the assumption that there is no climate change. CO_2-eq = CO_2-equivalents.

decline in the CO_2 production because of a decrease in the respiration rate (Kludze *et al*., 1993). In the DNDC model, the oxygen required for the decomposition of SOC to humus, litter, and DOC is calculated in proportion to the mass of the roots during flooding (Fumoto *et al*., 2008). The results of the DNDC model also showed that root growth in the 2090s would decrease by 8.1% and 10.2% with 10- and 30-cm tillage (data not shown here), respectively, compared to the 2020s, which is in agreement with the decline in CO_2 emissions.

Meanwhile, the national CH_4 emissions would increase at a higher rate, in spite of the gradual depletion of SOC stocks under the RCP-8.5 scenario. For example, with a 30-cm tillage depth, CH_4 emissions would increase by 73.2% from 8.6×10^6 t CO_2-eq $year^{-1}$ in the 2020s to 14.9×10^6 t CO_2-eq $year^{-1}$ in the 2090s. As noted earlier, the CH_4 production is a result of methanogenic fermentation with a C source, and the activity of methanogenesis exhibits a strong positive correlation with temperature (Le Mer and Roger, 2001; Malyan *et al*., 2016). Therefore, it can be stated that for the two parameters that have an opposite effect on CH_4 emission, the impact of temperature rise overwhelms that of SOC depletion, thus leading to increased CH_4 emissions under the RCP-8.5 scenario in the 2090s.

Limitations and implications of this study

The accuracy of the high-resolution prediction model is strongly dependent on the quality of the input data (Lugato *et al*., 2010). The performance of the DNDC model

was assessed through verification with field measurements. However, there were a couple of limitations related to the quality of the input data, which might inevitably lead to uncertainty in the model prediction.

Firstly, because the DNDC model predictions were made on the basis of high-resolution (1 km^2) soil and weather data, highly accurate GHG estimations were expected. However, the model was run using the average soil data per grid cell. If the DNDC model was run with the minimum/maximum soil input data from each grid, the uncertainty of the model prediction would be reduced. Therefore, the minimum/maximum soil data for each grid should be constructed and applied for more accurate model predictions.

Secondly, the common agronomic practices for rice cultivation recommended by the KRDA (crop data, the level and timing of fertilization, *etc*.) were employed, as it is very difficult to collect the data of agronomic practices actually applied in each grid cell. The amount, timing, and type (*e.g*., organic or chemical) of fertilizer might have a significant effect on the model prediction of GHG emissions (Chen *et al*., 2016). In addition, the calibration of the crop data in the performance highly affects the accuracy of the results (Hastings *et al*., 2010). The results of this study were based on crop data (*e.g*., maximum crop yield and water demand) obtained from typical *japonica* rice that is generally cultivated in South Korea. Therefore, to reduce the uncertainty, a government-driven commitment to collect agronomic practice and crop data from regional administrative units is desired.

Meanwhile, national GHG emissions can be estimated using Tier 1, 2, or 3 methodologies: Tier 1 relies on a widespread emission factor; Tier 2 utilizes a country-specific emission factor; and Tier 3 encompasses direct measurement and modeling approaches through national application (Reay *et al*., 2012). In the USA, Tier 3 N_2O emissions have already been estimated based on weather data with a resolution of 1 km^2, national-level soil data and agronomic practices data (USEPA, 2013). Until now, South Korea has been assessing CH_4 emissions in rice paddy fields utilizing the Tier 2 country-specific emission factors (GIR, 2015). Thus, the results of this study (national CO_2 and CH_4 emissions) are meaningful, since this work is the first application of a Tier 3 modeling approach to paddy fields in South Korea using 1-km^2 scale weather and soil data. More accurate Tier 3 GHG estimates can be performed when minimum/maximum soil data, agronomic practices data, and crop data are collected and used as input data.

CONCLUSIONS

The objective of this study was to estimate the CO_2 and CH_4 emissions from entire paddy fields in South Korea under the climate change scenario RCP-8.5. This estimation was made using the DNDC model with weather and soil data at a resolution of 1 km^2, between the 2020s and 2090s. In the absence of climate change, national CO_2 and CH_4 emissions would exhibit no significant differences between the 2020s and 2090s, ranging 5.8×10^6–6.0×10^6 and 6.4×10^6–6.6×10^6 t CO_2-eq $year^{-1}$, respectively. Under the RCP-8.5 scenario, however, the emissions of CH_4 in the 2090s would increase by 72.6% and 73.2% with the practice of 10- and 30-cm-deep tillage, respectively, compared to the 2020s. On the other hand, the emissions of CO_2 would decrease steadily under the same circumstances, most likely due to a reduced oxygen demand by the rice root system and the depletion of SOC stocks in paddy soils. The emissions of CH_4 from paddy fields can be greatly attenuated by intermittent flooding, while the CO_2 emissions were less influenced by this. In the 2090s, the differences in the regional SOC stocks and local temperatures are mainly responsible for the emissions of CO_2 and CH_4, respectively. The results of this work indicate that the emission inventory of CO_2 and CH_4 from paddy fields in South Korea can be documented by the results of the DNDC model prediction. In addition, based on the information on the causative relationship between agronomic factors (tillage and flooding) and GHG emissions, appropriate management of national emissions of CO_2 and CH_4, originating from all paddy fields in South Korea, can be executed in the face of climate change.

ACKNOWLEDGEMENT

This study was funded in part by the Korea Ministry of Environment (MOE) *via* the Climate Change Correspondence Program (No. 2014-001310008) and in part by Korea University Grant.

SUPPLEMENTARY MATERIAL

Supplementary material for this article can be found in the online version.

REFERENCES

Arai-Sanoh Y, Ishimaru T, Ohsumi A, Kondo M. 2010. Effects of soil temperature on growth and root function in rice. *Plant Prod Sci*. **13**: 235–242.

Aulakh M S, Wassmann R, Bueno C, Rennenberg H. 2001. Impact of root exudates of different cultivars and plant development stages of rice (*Oryza sativa* L.) on methane production in a paddy soil. *Plant Soil*. **230**: 77–86.

Chen H, Yu C Q, Li C S, Xin Q C, Huang X, Zhang J, Yue Y L, Huang G R, Li X C, Wang W. 2016. Modeling the impacts of water and fertilizer management on the ecosystem service of rice rotated cropping systems in China. *Agric Ecosyst Environ*. **219**: 49–57.

Chun J A, Shim K M, Min S H, Wang Q. 2016. Methane mitigation for flooded rice paddy systems in South Korea using a process-based model. *Paddy Water Environ*. **14**: 123–129.

Davidson E A, Janssens I A. 2006. Temperature sensitivity of soil carbon decomposition and feedbacks to climate change. *Nature*. **440**: 165–173.

Food and Agriculture Organization (FAO). 2012. FAOSTAT Database. Available online at http://fao.org/faostat/en/#home (verified on October 18, 2018).

Fumoto T, Kobayashi K, Li C S, Yagi K, Hasegawa T. 2008. Revising a process-based biogeochemistry model (DNDC) to simulate methane emission from rice paddy fields under various residue management and fertilizer regimes. *Glob Chang Biol*. **14**: 382–402.

Greenhouse Gas Inventory and Research Center (GIR). 2015. National Greenhouse Gas Inventory Report of Korea (in Korean). Available online at http://www.gir.go.kr/home/index.do?menuId=36 (verified on October 18, 2018).

Gutierrez J, Kim S Y, Kim P J. 2013. Effect of rice cultivar on CH_4 emissions and productivity in Korean paddy soil. *Field Crop Res*. **146**: 16–24.

Haque M M, Kim S Y, Ali M A, Kim P J. 2015. Contribution of greenhouse gas emissions during cropping and fallow seasons on total global warming potential in mono-rice paddy soils. *Plant Soil*. **387**: 251–264.

Hastings A F, Wattenbach M, Eugster W, Li C S, Buchmann N, Smith P. 2010. Uncertainty propagation in soil greenhouse gas emission models: An experiment using the DNDC model and at the Oensingen cropland site. *Agric Ecosyst Environ*. **136**: 97–110.

Hillel D. 1998. Environmental Soil Physics: Fundamentals, Applications, and Environmental Considerations. Academic Press, San Diego.

Huang S, Sun Y N, Yu X C, Zhang W J. 2016. Interactive effects of temperature and moisture on CO_2 and CH_4 production in a paddy soil under long-term different fertilization regimes. *Biol Fertil Soils*. **52**: 285–294.

Intergovernmental Panel on Climate Change (IPCC). 2007. Climate Change 2007: Synthesis Report. Contribution of Working Groups I, II and III to the Fourth Assessment Report of the Intergovernmental Panel on Climate Change. IPCC, Geneva.

Intergovernmental Panel on Climate Change (IPCC). 2013. Climate Change 2013: The Physical Science Basis. Contribution of Working Group I to the Fifth Assessment Report of the Intergovernmental Panel on Climate Change. Cambridge University Press, Cambridge and New York.

Jansson P E, Moon D S. 2001. A coupled model of water, heat and mass transfer using object orientation to improve flexibility and functionality. *Environ Model Softw*. **16**: 37–46.

Kludze H K, DeLaune R D, Patrick W H Jr. 1993. Aerenchyma formation and methane and oxygen exchange in rice. *Soil Sci Soc Am J*. **57**: 386–391.

Korean Statistical Information Service (KOSIS). 2012. Korean Statistical Information Service, Daejeon. Available online at http://kosis.kr (verified on October 18, 2018).

Le Mer J, Roger P. 2001. Production, oxidation, emission and consumption of methane by soils: A review. *Eur J Soil Biol*. **37**: 25–50.

Li C S, Frolking S, Frolking T A. 1992. A model of nitrous oxide evolution from soil driven by rainfall events: 1. Model structure and sensitivity. *J Geophys Res Atmos*. **97**: 9759–9776.

Li H, Qiu J J, Wang L G, Yang L. 2011. Advance in a terrestrial biogeochemical model-DNDC model. *Acta Ecol Sin*. **31**: 91–96.

Lugato E, Zuliani M, Alberti G, Vedove G D, Gioli B, Miglietta F, Peressotti A. 2010. Application of DNDC biogeochemistry model to estimate greenhouse gas emissions from Italian agricultural areas at high spatial resolution. *Agric Ecosyst Environ*. **139**: 546–556.

Malyan S K, Bhatia A, Kumar A, Gupta D K, Singh R, Kumar S S, Tomer R, Kumar O, Jain N. 2016. Methane production, oxidation and mitigation: A mechanistic understanding and comprehensive evaluation of influencing factors. *Sci Total Environ*. **572**: 874–896.

Marchetti A, Piccini C, Francaviglia R, Mabit L. 2012. Spatial distribution of soil organic matter using geostatistics: A key indicator to assess soil degradation status in central Italy. *Pedosphere*. **22**: 230–242.

Minamikawa K, Fumoto T, Itoh M, Hayano M, Sudo S, Yagi K. 2014. Potential of prolonged midseason drainage for reducing methane emission from rice paddies in Japan: A long-term simulation using the DNDC-Rice model. *Biol Fertil Soils*. **50**: 879–889.

Omran E S E. 2012. Improving the prediction accuracy of soil mapping through geostatistics. *Int J Geosci*. **3**: 574–590.

Osunbitan J A, Oyedele D J, Adekalu K O. 2005. Tillage effects on bulk density, hydraulic conductivity and strength of a loamy sand soil in southwestern Nigeria. *Soil Tillage Res*. **82**: 57–64.

Parton W J, Mosier A R, Ojima D S, Valentine D W, Schimel D S, Weier K, Kulmala A E. 1996. Generalized model for N_2 and N_2O production from nitrification and denitrification. *Global Biogeochem Cycles*. **10**: 401–412.

Pathak H, Li C, Wassmann R. 2005. Greenhouse gas emissions from Indian rice fields: Calibration and upscaling using the DNDC model. *Biogeosci Discuss*. **2**: 77–102.

Reay D S, Davidson E A, Smith K A, Smith P, Melillo J M, Dentener F, Crutzen P J. 2012. Global agriculture and nitrous oxide emissions. *Nat Clim Chang*. **2**: 410–416.

Snyder C S, Bruulsema T W, Jensen T L, Fixen P E. 2009. Review of greenhouse gas emissions from crop production systems and fertilizer management effects. *Agric Ecosyst Environ*. **133**: 247–266.

United States Environmental Protection Agency (USEPA). 2013. Inventory of U.S. greenhouse gas emissions and sinks: 1990–2011. Available online at https://www.epa.gov/ghgemissions/inventory-us-greenhouse-gas-emissions-and-sinks-1990–2011 (verified on October 18, 2018).

Vaezi A R. 2014. Modeling runoff from semi-arid agricultural lands in Northwest Iran. *Pedosphere*. **24**: 595–604.

Yang S S, Chang H L. 2001. Effect of green manure amendment and flooding on methane emission from paddy fields. *Chemosph: Global Change Sci*. **3**: 41–49.

Zhou Y L, Sun B. 2017. Nitrogen use efficiency of rice under cadmium contamination: Influence of rice cultivar versus soil type. *Pedosphere*. **27**: 1092–1104.